Japanese Journal of Applied Physics **52** (2013) 01AK04 **REGULAR PAPER**
http://dx.doi.org/**10.7567/JJAP.52.01AK04**

Fabrication of Graphene-Based Films Using Microwave-Plasma-Enhanced Chemical Vapor Deposition

Mineo Hiramatsu[1], Masateru Naito[1], Hiroki Kondo[2], and Masaru Hori[2]

[1]*Department of Electrical and Electronic Engineering, Meijo University, Nagoya 468-8502, Japan*
[2]*Department of Electrical Engineering and Computer Science, Nagoya University, Nagoya 464-8603, Japan*

Received April 30, 2012; revised October 11, 2012; accepted October 15, 2012; published online January 21, 2013

Microwave plasma is one of the high-density plasmas and has been extensively used for the growth of diamond and aligned carbon nanotubes for more than a decade. However, the conventional microwave plasma of the cylindrical resonant cavity type is not suitable for the synthesis of graphene. The plasma ball produced in the resonant cavity provides a number of important species as well as ions, while deposits are damaged by the excess ion bombardment since the substrate is exposed to the plasma ball. To simply control the position of the plasma ball and reduce the ion bombardment on the substrate surface, a grounded molybdenum mesh was installed over the substrate plate to realize a remote plasma configuration. As a result, the distance between the plasma ball and the copper substrate was increased, and few-layer graphene-based films were successfully synthesized in 1 min on copper substrates placed on the entire region of a substrate holder 10 cm in diameter by using conventional microwave-plasma enhanced chemical vapor deposition.

1. Introduction

Graphene, which has a hexagonal arrangement of carbon atoms forming a one-atom-thick planar sheet, is a promising material for future electronic applications owing to its high electrical conductivity, as well as its chemical and physical stability.[1)] However, the large-scale synthesis of high-quality graphene represents a bottleneck for next-generation graphene devices. Graphene has been synthesized using various methods including (i) mechanical exfoliation from highly oriented pyrolytic graphite (HOPG),[2,3)] (ii) chemical exfoliation from bulk graphite,[4–7)] (iii) thermal decomposition of carbon-terminated silicon carbide (SiC),[8,9)] and (iv) thermal chemical vapor deposition (CVD) on metals such as nickel (Ni) and copper (Cu) substrates at high substrate temperatures of up to 1000 °C.[10–16)] In the case of the thermal CVD of graphene on a Ni substrate, thermally decomposed carbon atoms dissolved owing to the high solubility of carbon in Ni at high temperatures, and segregation to form graphene occurred during cooling to room temperature at an appropriate rate.[10)] In the case of thermal CVD on a Cu substrate, on the other hand, carbon atoms did not dissolve into Cu owing to the very low solubility of carbon in Cu,[17)] while the coverage of the surface with surface-migrating carbon adatoms proceeded, resulting in the formation of graphene.[13)]

Plasma-enhanced CVD (PCVD) is among the early methods of synthesizing a few layers of vertically standing graphene or carbon nanowalls.[18–22)] PCVD is becoming one of the most promising techniques for the production of diamond, aligned carbon nanotube films, and carbon nanowalls, owing to its feasibility and potentiality for large-area production with reasonable growth rates at relatively low temperatures. To date, vertical layered-graphene sheets and carbon nanowalls have been grown using various PCVD methods employing microwave plasma, radio-frequency (rf) inductively coupled plasma (ICP), rf capacitively coupled plasma (CCP) with H radical injection, very high frequency (VHF) plasma with H radical injection, and electron-beam-excited plasma,[18–22)] where the substrates were exposed to the plasma. On the other hand, the synthesis of planar graphene films on the substrates has been reported recently.[23–27)] Yuan et al. reported the synthesis of graphene using microwave-plasma-enhanced CVD (MWPCVD).[23)] As a matter of fact, graphene was found in the black product deposited on the wall of a stainless-steel cylinder surrounding the substrate holder under the plasma ball region. It is noted that the growth region of graphene was not directly exposed to the plasma ball in their method. Nandamuri et al. have grown a graphene film on a Ni substrate by rf (13.56 MHz) PCVD with a remote plasma configuration at 650–700 °C in about 1 min.[24)] In the case of PCVD on Ni, an appropriate cooling process is still important for carbon segregation. Very recently, Kim et al. have reported the low-temperature synthesis of large-area graphene-based films using surface wave plasma-enhanced CVD (SWPCVD) on Cu and aluminum (Al) foils at substrate temperatures below 400 °C.[27)] The SWP provides high-density plasmas and radicals and has a relatively low electron temperature (below 2 eV) and also a low plasma space potential (below 10 V) in the bulk region even at low gas pressures.[27,28)] Therefore, the SWP can reduce ion bombardment on the substrate surface, resulting in the low-temperature synthesis of graphene-based films, although the deposited film is the accumulation of few-layer graphene nanoflakes and its sheet resistance is high.

Microwave plasma is one of the high-density plasmas and is suitable for decomposing H_2 molecules to generate H atoms effectively. Two types of MWPCVD, called the NIRIM (National Institute of Research of Inorganic Materials, Japan) type and ASTeX (Applied Science and Technology, Inc.) type, have been extensively used for the growth of diamond films and aligned carbon nanotubes (CNTs) for more than a decade. In the case of the NIRIM-type MWPCVD system, the CH_4/H_2 plasma is generated in a cylindrical quartz tube, which intersects a rectangular waveguide. The size of the substrate is limited to approximately 5–10 cm^2 by the inner diameter of the cylindrical quartz tube. On the other hand, the ASTeX-type reactor consists of a cylindrical stainless-steel chamber as a resonant cavity. A microwave (2.45 GHz) is coupled from a rectangular waveguide into the resonant cavity via an axial antenna. A discharge called a *plasma ball* is generated above the substrate. The plasma ball heats the substrate. In this

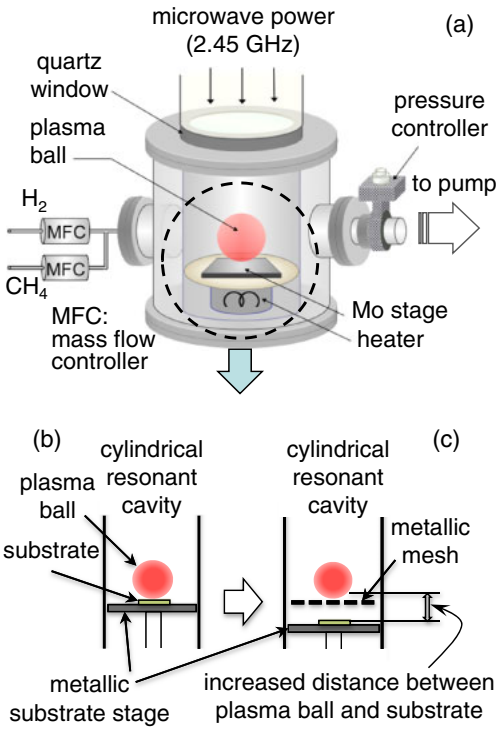

Fig. 1. (Color online) (a) Schematic of conventional MWPCVD system of cylindrical resonant cavity type. Enlarged views in the vicinity of substrate holder relative to the plasma ball, (b) "type I configuration", where substrate is exposed to plasma ball, and (c) "type II configuration", where grounded Mo mesh is installed over the substrate holder.

system, the CVD process is operated at pressures of 20–80 Torr ($\sim 10^3$ Pa), and the reactor pressure and microwave power cannot be varied completely independently. The conventional microwave plasma of the cylindrical resonant cavity type is not suitable for the synthesis of graphene. The plasma ball provides a number of important species as well as ions, while deposits are damaged by the excess ion bombardment since the substrate is exposed to the plasma ball. In this work, we attempted to fabricate graphene films on a Cu substrate at temperatures of approximately 800 °C using MWPCVD, which has been used to grow diamond and aligned CNT films.[29,30] In the present CVD system, by simply installing a grounded molybdenum (Mo) mesh over the substrate plate, the distance between the plasma ball and the Cu substrate was increased, reducing the ion bombardment on the substrate surface. We have successfully fabricated graphene-based films on a Cu substrate using conventional MWPCVD, by controlling the position of the plasma ball.

2. Experiments

In the case of conventional MWPCVD of the cylindrical resonant cavity type, which is defined as the "type I configuration" in the present study, a microwave (2.45 GHz) is coupled from a rectangular waveguide into the cavity via an axial antenna, and a discharge called a plasma ball is generated above the substrate, as shown in Figs. 1(a) and 1(b). The plasma ball provides a number of important species, while deposits are damaged by the excess ion bombardment since the substrate is exposed to the plasma ball. As shown in Fig. 1(c), the present CVD system with the "type II configuration" has a grounded Mo mesh installed between the plasma ball and the substrate plate to realize a remote plasma configuration by increasing the distance between the plasma ball and the substrate, resulting in the reduction of ion bombardment on the substrate surface. The typical distance between the grounded Mo mesh and the substrate plate was 2 cm. In our experiments, commercially available polycrystalline Cu sheets with a thickness of 0.5 mm and purity >99.96% from The Nilaco Corporation were cut into 1×1 cm^2 pieces for the use as Cu substrates without pretreatment. A mixture of CH_4 and H_2 was used as the source gas. The flow rates of CH_4 and H_2 were 20 and 180 sccm, respectively. The growth experiments were carried out for 1–5 min at a microwave power of 1300 W, a total pressure of 80 Torr, and a substrate temperature of 880 °C. During the growth process, the substrate temperature was monitored using a radiation thermometer. At the fixed heater temperature, the substrate temperature was decreased to about 50 °C by increasing the distance between the plasma ball and the substrate in the case of the type II configuration. Therefore, the substrate temperature was kept at 800 °C for both cases by controlling the heater temperature. Deposits on the Cu substrate were evaluated by scanning electron microscopy (SEM) and transmission electron microscopy (TEM). Raman spectra were measured for the deposits using a 514.5 nm line of an argon laser.

3. Results and Discussion

In the case of CVD using the conventional microwave plasma of the cylindrical resonant cavity type (type I configuration) shown in Fig. 1(b), a vertically aligned CNT film is grown on a Co-catalyzed Si substrate.[30] Without a catalyst under similar conditions, as shown in Fig. 2(a), carbon nanoflakes are grown in 5 min on a Si substrate placed at the center of the substrate holder. First, a deposition experiment was carried out on Cu substrates using the type I configuration. A graphene-based film was not formed on the Cu substrate placed at the center of the substrate holder, which was exposed to the plasma ball. On the Cu substrate placed at the edge of the substrate holder 10 cm in diameter, on the other hand, a graphene-based film was formed. Figure 2(b) shows a SEM image of an as-grown graphene-based film formed on a Cu substrate in 5 min using the type I configuration, where the Cu substrate was placed at the edge of the substrate holder. In Fig. 2(b), the dashed lines highlight wrinkles or domain boundaries of the graphene-based film, and the underlying microstructure (Cu grain boundaries) of the Cu substrate is clearly visible. The wrinkles are associated with the thermal expansion coefficient difference between Cu and graphene.[13] The graphene wrinkles or graphene domain boundaries are found to cross Cu grain boundaries, indicating that the weak interaction between graphene and the Cu substrate allows the graphene domains to expand over the Cu grain boundaries. In contrast, in the case of CVD using the type II configuration, it was confirmed that graphene-based films were grown on Cu substrates placed on the entire region of the substrate holder. The morphology of the graphene-based films grown on the Cu substrates using the type II configuration was similar to that shown in Fig. 2(b).

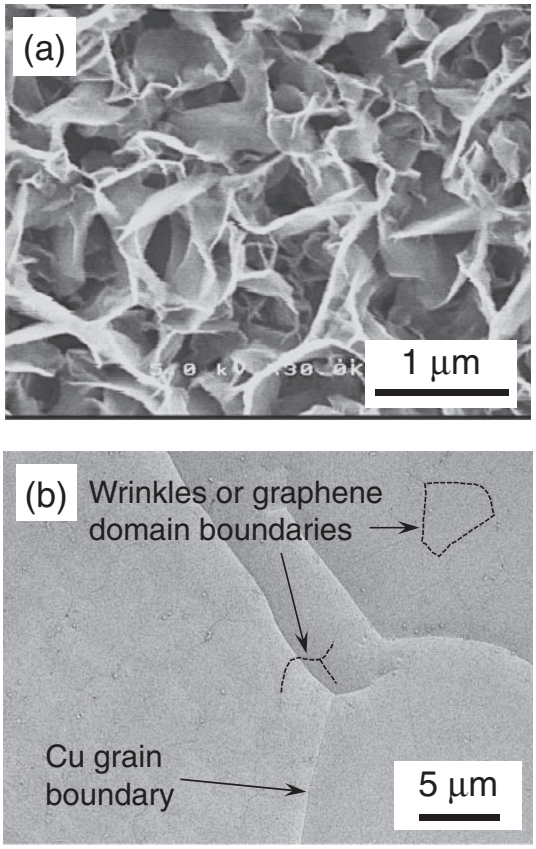

Fig. 2. (a) SEM image of carbon nanoflakes grown in 5 min on the Si substrate placed at the center of the substrate holder using type I configuration. (b) SEM image of as-grown graphene-based film on the Cu substrate in 5 min using type I configuration, where the Cu substrate was placed at the edge of substrate holder. The dashed lines highlight wrinkles or domain boundaries of the graphene-based film, and the underlying Cu grain boundaries are clearly visible.

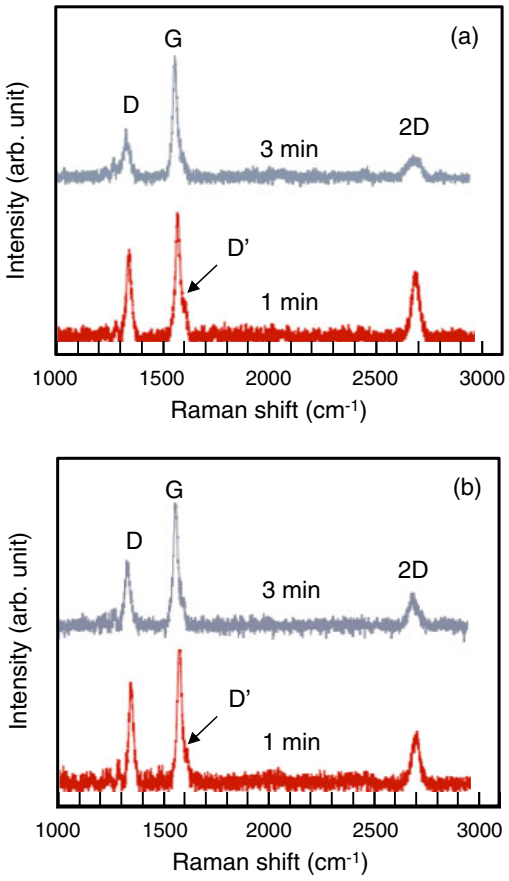

Fig. 3. (Color online) Raman spectra of graphene-based films grown using type II configuration on Cu substrates for 1 and 3 min. Cu substrates were placed at the edge (a) and the center (b) of the substrate holder 10 cm in diameter.

Raman spectroscopy characterization was performed for the graphene-based films grown using the type II configuration. Raman spectra were taken for the films grown on the Cu substrates placed at the center and edge of the substrate holder 10 cm in diameter. Figure 3(a) shows Raman spectra of graphene-based films grown for 1 and 3 min on Cu substrates placed at the edge of the holder. The Raman spectra of the films show three peaks centered at 1350, 1580, and 2690 cm^{-1}, which are assigned to the D, G, and 2D bands, respectively. The strong G band peak indicates the formation of a graphitized structure. The D band peak corresponds to the disorder-induced phonon mode, which is attributed to the defects or structural disorder in graphenes. In the Raman spectrum of the film synthesized for 1 min, the G band peak is accompanied by a shoulder peak at 1620 cm^{-1} (D′ band), which is associated with finite-size graphite crystals and graphene edges.[31,32] The most prominent feature in the Raman spectrum of graphene is the 2D band peak. The 2D band peak is used to confirm the presence of graphene, and it originates from a double resonance process that links phonons to the electronic band structure. The position and shape of the 2D band peak are known to distinguish the number of graphene layers. Moreover, the intensity ratio of the 2D to G band peaks has a good correlation with the number of graphene layers.[33,34] The intensity ratio of the 2D band peak to the G band peak (I_{2D}/I_G) in the Raman spectrum of graphene increases with decreasing number of graphene layers.[11,35,36] In the Raman spectrum of the graphene-based film grown for 3 min, the 2D band peak was broad and its intensity was small. In the Raman spectrum of the graphene-based film grown for 1 min, on the other hand, the 2D band peak became sharp and its intensity increased, indicating the synthesis of a few-layer (>3) graphene sheet in the short period of 1 min. The relatively strong and sharp D band peak and D′ band shoulder peak suggest a more nanocrystalline structure and the presence of domain boundaries, which are a discontinuity in the sp^2-hybridized carbon atom network that forms the graphene sheet. Figure 3(b) shows Raman spectra of graphene-based films grown for 1 and 3 min on Cu substrates placed at the center of the substrate holder. The Raman spectra shown in Fig. 3(b) for the films grown at a position close to the plasma ball are almost identical to those for the films grown at the edge of the holder shown in Fig. 3(a), indicating that graphene-based films were grown on the entire region of the substrate holder 10 cm in diameter by using the type II configuration.

Figure 4 shows a cross-sectional TEM image of a graphene-based film grown using the type II configuration on a Cu substrate for 1 min. From the TEM observation shown in Fig. 4, the number of graphene layers was 7–8 in the case of the graphene-based film grown for 1 min. The

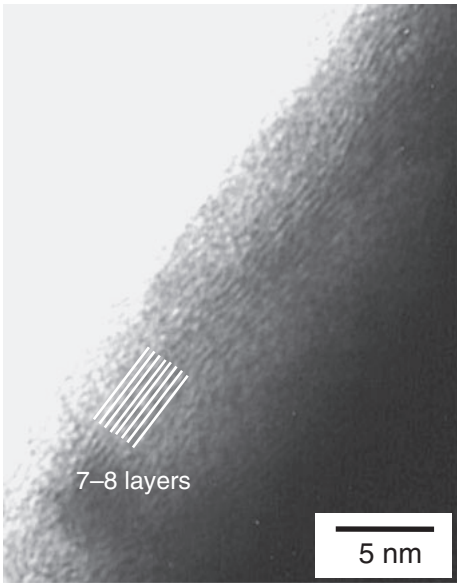

Fig. 4. Cross-sectional TEM image of graphene-based film grown using type II configuration on Cu substrate for 1 min.

synthesized graphene-based films were slightly defective and composed of partially damaged graphene layers, as seen from the TEM image in Fig. 4. As was indicated by the Raman-based analysis shown in Figs. 3(a) and 3(b), moreover, the relatively strong and sharp D band peak and D′ band shoulder peak suggested the structural disorder in graphenes and the presence of domain boundaries. From these considerations, we conclude that the deposited film was the accumulation of submicrometer-size few-layer graphene-based materials.

In the case of graphene growth through thermal CVD on a Cu substrate, graphene is grown by a surface-catalyzed process rather than by a precipitation process as reported for Ni.[10,11] The precursor for graphene formation mainly originates from a carbon-containing gas such as CH_4 that is catalytically decomposed on the heated Cu surface with minimal carbon diffusion into the Cu.[17] When the surface of the Cu substrate is fully covered with monolayer graphene, growth terminates because of the absence of a catalyst to decompose CH_4. Further exposure to the carbon source gas does not lead to the deposition of multilayer graphene.[16,37] Moreover, it has been reported that hydrogen plays a dual role in the process of graphene growth by thermal CVD on copper foil.[38] It acts as a cocatalyst in forming active surface-bound carbon species required for graphene growth and controls the grain shape and dimensions by etching away the weak carbon–carbon bonds. Graphene nucleation, the growth rate, and the termination size of grains are affected by competition between these two processes related to hydrogen. In the case of PCVD, on the other hand, the carbon precursor is generated in the gas phase through the dissociation of the carbon source gas due to the electron impact. Accordingly, graphene growth can be attained in a short period at a relatively low temperature by PECVD in principle. In fact, the deposition of multilayer graphene with a defective structure and domain boundaries should proceed even after the full coverage with monolayer graphene. Very recently, Terasawa and Saiki have successfully grown graphene on a Cu substrate using capacitively coupled PECVD, where H and C_2 radicals are less abundant than in the conventional microwave plasma. It has been reported that in the case of graphene growth using PCVD, the catalytic nature of Cu affects the growth of monolayer graphene at high substrate temperatures, while the growth at low temperatures and the growth of multilayer graphene are mostly dominated by radicals generated in the plasma.[39] In particular, a number of carbon precursors such as C_2 radicals are generated in the microwave plasma, resulting in the formation of multilayer graphene with a high growth rate. In addition, the grain size of graphene was estimated to be approximately 20 nm from the Raman peak intensity ratio of the D band to the G band (I_D/I_G).[34] This small size of grain boundaries is considered to be due to the high density of carbon precursors as well as the ion bombardment on the growing surface. The ion bombardment should induce defects in the formed graphene. Furthermore, the ion bombardment should enhance the adsorption of the carbon precursor on the graphene, considering the similarity to fluorocarbon plasma, where the sticking coefficient of CF_3 radicals is increased by the ion bombardment, but is relatively low without the ion bombardment.[40] Thereby, the secondary nucleation should easily occur on the formed graphene, resulting in the formation of multilayer graphene with a defective structure and small grain boundaries. Meanwhile, excess ion bombardment will induce the nucleation of randomly oriented nanographenes to form carbon nanowalls or nanoflakes, as shown in Fig. 2(a). Therefore, to improve the crystallinity of graphene-based films, it is crucially important to control the flux and energy of ions irradiating the substrate surface. The nucleation density and size of graphene grain boundaries are affected by the surface morphology and thickness of the Cu substrate,[16] although after the nucleation, the graphene domains should grow without disruption above the Cu grain boundaries. The optimization of the position of the metal mesh, mesh spacing, and substrate biasing is under way. The simple method employed in the present study to realize the remote plasma configuration will be applicable to other plasmas including atmospheric pressure plasma, rf CCP, and ICP.

4. Conclusions

We have successfully fabricated graphene-based films on Cu substrates using conventional MWPCVD by controlling the position of the plasma ball. Thus far, the conventional microwave plasma of the cylindrical resonant cavity type has not been suitable for the synthesis of graphene. The plasma ball produced in the resonant cavity provides a number of important species as well as ions, while deposits are damaged by the excess ion bombardment since the substrate is exposed to the plasma ball. In the present study, to control the position of the plasma ball and reduce the ion bombardment on the substrate surface, we simply installed a grounded molybdenum mesh over the substrate plate to realize a remote plasma configuration. As a result, the distance between the plasma ball and the copper substrate was increased, and few-layer graphene-based films were successfully synthesized in 1 min on the copper substrates placed on the entire region of a substrate holder 10 cm in diameter.

1) A. K. Geim and K. S. Novoselov: Nat. Mater. **6** (2007) 183.
2) K. S. Novoselov, A. K. Geim, S. V. Morozov, D. Jiang, Y. Zhang, S. V. Dubonos, I. V. Grigorieva, and A. A. Firsov: Science **306** (2004) 666.
3) X. Liang, Z. Fu, and S. Y. Chou: Nano Lett. **7** (2007) 3840.
4) G. Eda, G. Fanchini, and M. Chhowalla: Nat. Nanotechnol. **3** (2008) 270.
5) X. Li, G. Zhang, X. Bai, X. Sun, X. Wang, E. Wang, and H. Dai: Nat. Nanotechnol. **3** (2008) 538.
6) H. A. Becerril, J. Mao, Z. Liu, R. M. Stoltenberg, Z. Bao, and Y. Chen: ACS Nano **2** (2008) 463.
7) X. Wang, L. Zhi, and K. Müllen: Nano Lett. **8** (2008) 323.
8) T. Ohta, A. Bostwick, T. Seyller, K. Horn, and E. Rotenberg: Science **313** (2006) 951.
9) C. Berger, Z. M. Song, X. B. Li, X. S. Wu, N. Brown, C. Naud, D. Mayo, T. B. Li, J. Hass, A. N. Marchenkov, E. H. Conrad, P. N. First, and W. A. de Heer: Science **312** (2006) 1191.
10) Q. Yu, J. Lian, S. Siriponglert, H. Li, Y. P. Chen, and S. S. Pei: Appl. Phys. Lett. **93** (2008) 113103.
11) A. Reina, X. Jia, J. Ho, D. Nezich, H. Son, V. Bulovic, M. S. Dresselhaus, and J. Kong: Nano Lett. **9** (2009) 30.
12) X. Li, Y. Zhu, W. Cai, M. Borysiak, B. Han, D. Chen, R. D. Piner, L. Colombo, and R. S. Ruoff: Nano Lett. **9** (2009) 4359.
13) X. Li, W. Cai, J. An, S. Kim, J. Nah, D. Yang, R. Piner, A. Velamakanni, I. Jung, E. Tutuc, S. K. Banerjee, L. Colombo, and R. S. Ruoff: Science **324** (2009) 1312.
14) Y. Lee, S. Bae, H. Jang, S. Jang, S.-E. Zhu, S. H. Sim, Y. I. Song, B. H. Hong, and J.-H. Ahn: Nano Lett. **10** (2010) 490.
15) Y. H. Lee and J. H. Lee: Appl. Phys. Lett. **96** (2010) 083101.
16) C. Mattevi, H. Kima, and M. Chhowalla: J. Mater. Chem. **21** (2011) 3324.
17) G. A. López and E. J. Mittemeijer: Scr. Mater. **51** (2004) 1.
18) Y. H. Wu, P. W. Qiao, T. C. Chong, and Z. X. Shen: Adv. Mater. **14** (2002) 64.
19) J. J. Wang, M. Y. Zhu, R. A. Outlaw, X. Zhao, D. M. Manos, B. C. Holloway, and V. P. Mammana: Appl. Phys. Lett. **85** (2004) 1265.
20) M. Hiramatsu, K. Shiji, H. Amano, and M. Hori: Appl. Phys. Lett. **84** (2004) 4708.
21) S. Kondo, M. Hori, K. Yamakawa, S. Den, H. Kano, and M. Hiramatsu: J. Vac. Sci. Technol. B **26** (2008) 1294.
22) T. Mori, M. Hiramatsu, K. Yamakawa, K. Takeda, and M. Hori: Diamond Relat. Mater. **17** (2008) 1513.
23) G. D. Yuan, W. J. Zhang, Y. Yang, Y. B. Tang, Y. Q. Li, J. X. Wang, X. M. Meng, Z. B. He, C. M. L. Wu, I. Bello, C. S. Lee, and S. T. Lee: Chem. Phys. Lett. **467** (2009) 361.
24) G. Nandamuri, S. Roumimov, and R. Solanki: Appl. Phys. Lett. **96** (2010) 154101.
25) J. L. Qi, W. T. Zheng, X. H. Zheng, X. Wang, and H. W. Tian: Appl. Surf. Sci. **257** (2011) 6531.
26) J. H. Kim, E. J. D. Castro, Y. G. Hwang, and C. H. Lee: J. Korean Phys. Soc. **58** (2011) 53.
27) J. Kim, M. Ishihara, Y. Koga, K. Tsugawa, M. Hasegawa, and S. Iijima: Appl. Phys. Lett. **98** (2011) 091502.
28) J. Kim, K. Tsugawa, M. Ishihara, Y. Koga, and M. Hasegawa: Plasma Sources Sci. Technol. **19** (2010) 015003.
29) M. Hiramatsu, K. Kato, C. H. Lau, J. S. Foord, and M. Hori: Diamond Relat. Mater. **12** (2003) 365.
30) M. Hiramatsu, H. Nagao, M. Taniguchi, H. Amano, Y. Ando, and M. Hori: Jpn. J. Appl. Phys. **44** (2005) L693.
31) R. J. Nemanich and S. A. Solin: Phys. Rev. B **20** (1979) 392.
32) S. Kurita, A. Yoshimura, H. Kawamoto, T. Uchida, K. Kojima, M. Tachibana, P. Molina-Morales, and H. Nakai: J. Appl. Phys. **97** (2005) 104320.
33) A. C. Ferrari, J. C. Meyer, V. Scardaci, C. Casiraghi, M. Lazzeri, F. Mauri, S. Piscanec, D. Jiang, K. S. Novoselov, S. Roth, and A. K. Geim: Phys. Rev. Lett. **97** (2006) 187401.
34) A. C. Ferrari: Solid State Commun. **143** (2007) 47.
35) Z. H. Ni, H. M. Wang, J. Kasim, H. M. Fan, T. Yu, Y. H. Wu, Y. P. Feng, and Z. X. Shen: Nano Lett. **7** (2007) 2758.
36) K. S. Kim, Y. Zhao, H. Jang, S. Y. Lee, J. M. Kim, K. S. Kim, J.-H. Ahn, P. Kim, J.-Y. Choi, and B. H. Hong: Nature **457** (2009) 706.
37) X. Li, W. Cai, L. Colombo, and R. S. Ruoff: Nano Lett. **9** (2009) 4268.
38) I. Vlassiouk, M. Regmi, P. Fulvio, S. Dai, P. Datskos, G. Eres, and S. Smirnov: ACS Nano **5** (2011) 6069.
39) T. Terasawa and K. Saiki: Carbon **50** (2012) 869.
40) T. Tatsumi, Y. Hikosaka, S. Morishita, M. Matsui, and M. Sekine: J. Vac. Sci. Technol. A **17** (1999) 1562.